Open access • Journal Article • DOI:10.1088/0741-3335/52/2/025002

On the requirements to control neoclassical tearing modes in burning plasmas

Olivier Sauter, M. A. Henderson, G. Ramponi, H. Zohm ...+1 more authors

Institutions: École Polytechnique Fédérale de Lausanne, Max Planck Society

Published on: 01 Feb 2010 - Plasma Physics and Controlled Fusion (Institute of Physics and IOP Publishing Limited)

Topics: Bootstrap current

On the Requirements to Control Neoclassical Tearing Modes in Burning Plasmas

O. Sauter, M.A. Henderson, G. Ramponi[1], H. Zohm[2], C. Zucca*

Centre de Recherches en Physique des Plasmas,

Association EURATOM-Confédération Suisse,

EPFL, PPB-Ecublens, 1015 Lausanne, Switzerland

[1]*Istituto di Fisica del Plasma, EURATOM-ENEA-CNR Association, 20125 Milano, Italy*

[2]*IPP-Garching, Max Planck-Institute für Plasmaphysik, D-85748 Garching, Germany*

(Dated: November 10, 2009)

Abstract

Neoclassical tearing modes (NTMs) are magnetic islands which increase locally the radial transport and therefore degrade the plasma performance. They are self-sustained by the bootstrap current perturbed by the enhanced radial transport. The confinement degradation is proportional to the island width and to the position of the resonant surface. The q=2 NTMs are much more detrimental to the confinement than the 3/2 modes due to their larger radii. NTMs are metastable in typical scenarios with $\beta_N \geq 1$ and in the region where the safety factor is increasing with radius. This is due to the fact that the local perturbed pressure gradient is sufficient to self-sustain an existing magnetic island. The main questions for burning plasmas are whether there is a trigger mechanism which will destabilize NTMs, and what is the best strategy to control/avoid the modes. The latter has to take into account the main aim which is to maximize the Q factor, but also the controllability of the scenario. Standardized and simplified equations are proposed to enable easier prediction of NTM control in burning plasmas from present experimental results. The present expected requirements for NTM control with localised ECCD (electron cyclotron current drive) in ITER are discussed in detail. Other aspects of the above questions are also discussed, in particular the role of partial stabilisation of NTMs, the possibility to control NTMs at small size with little ECH power and the differences between controlling NTMs at the resonant surface or controlling the main trigger source, for the standard scenario namely the sawteeth. It is shown that there is no unique best strategy, but several tools are needed to most efficiently reduce the impact of NTMs on burning plasmas.

*Electronic address: olivier.sauter@epfl.ch

I. INTRODUCTION

Neoclassical tearing modes (NTMs) have been observed in many tokamaks [1, 2] and in particular in H-modes (high confinement modes) with monotonic safety factor (q) profiles. This is due to the low marginal beta above which NTMs are metastable [3]. In H-modes, the bootstrap fraction is increased and the perturbed bootstrap fraction due to the localized island is typically sufficient to sustain the island. The bootstrap current density is perturbed because of the local flattening of the pressure profile within the island, which also leads to a degradation of the confinement. The latter can be well estimated by the belt-model [4], yielding a relation between the island full width w and the degradation of the energy confinement time τ_e:

$$\frac{\Delta\tau_e}{\tau_e} = \Delta_\tau \, \frac{w_{sat}}{a}, \quad \text{with} \quad \Delta_\tau = 4\,\frac{\rho_s^3}{a^3}, \tag{1}$$

where w_{sat} is the saturated island width, ρ_s the radius of the resonant surface and a the plasma minor radius. NTMs can easily have island widths of 10% of the minor radius. With such a width and if the mode is localized near mid-radius, the confinement degradation is of the order of 5%. However if the mode is near $\rho_s/a = 0.8$, the degradation is about 20%. This is why 2/1 NTMs, at q=2, have much stronger impact on the plasma performance and clearly need to be avoided. Higher m/n modes, where m, n are the poloidal and toroidal mode numbers respectively, are located closer to the center and therefore have smaller impact on the global plasma performance. This is why one might allow such modes to exist, although even 4/3 modes have been observed to lead up to 10% degradation in the JET tokamak [5]. Note that the island size can increase significantly if the mode locks and therefore lead top larger confinement degradation [6–8].

Since NTMs are driven by a deficit of current density within the island, the easiest way to stabilize them is by adding localized current with electron cyclotron current drive (ECCD) in the island [9]-[18]. Recently, a cross-machine comparison of ECCD stabilised NTMs has allowed the prediction of the typical behavior expected in ITER [19]. It is shown that a driven current density of the order of the local bootstrap current density should be sufficient to fully stabilize the mode, $j_{cd}/j_{bs} \sim 1$, depending on the assumed model for the stabilizing mechanism at small island size as will be discussed below. Such a criteria is important for the design of the EC launcher in ITER [20]-[22]. The range of validity of such a criteria is also important and it will be discussed in detail in Sec. IV. The aiming accuracy and

related issues, as well as the question of the 2/1 mode locking, have been analysed in Ref. [7] and will not be analysed in details here, except with regards to the global strategy for NTM mitigation.

Another important aspect is the question of the existence of NTMs in burning plasmas and the onset criteria. It has been demonstrated in JET that the main trigger mechanism in low beta plasmas is the sawtooth crash [23]. It is also shown that crashes after long sawtooth period easily trigger NTMs, even at very low beta near the marginal beta limit. Since fast particles are very efficient to stabilize sawteeth [24]-[25], it is assumed here that the main condition for the existence of NTMs in sawtoothing burning plasmas will be related to the sawtooth activity. Therefore the control of sawteeth is inherantly part of any NTM control strategy. This will be discussed in Sec. VI. Note that for the other scenarios, hybrid and advanced, NTMs typically occur at much higher β_N values, close to the ideal limit, and both β_N and q profiles influence the onset conditions.

Other aspects related to NTMs and plasma performance are important. First the optimisation should be related to the factor Q, the ratio between the fusion and the auxiliary power. This factor characterizes the overall performance of a burning plasma. Since the stabilisation of NTMs with ECCD tends to decrease Q, by increasing the auxiliary power, an optimum Q might be obtained with partial stabilisation of the NTM. Another parameter is the relation between the time required to fully stabilize an NTM and the sawtooth period (or rather the time between successive NTM triggers). Finally the possibility to use preemptive ECCD (ECCD applied before the NTM onset) to optimize the power required for NTM stabilisation will also be discussed.

The paper is organized as follows, in Sec. II we present the main operational diagram relevant for NTM control in burning plasmas, namely the dependence of Q on additional EC power. In Sec. III the main equations for comparison with experiments and for the basis for predictions are presented, in Sec. IV the criteria $\eta_{NTM} = j_{cd}/j_{bs}$ for full stabilisation is analyzed, in Sec. V predictions for Q and partial stabilisation are presented, and in Sec. VI the strategy with respect to sawteeth activity and preemptive ECCD is discussed. Sec. VII concludes this paper.

II. BURNING PLASMA CONDITIONS

In order to discuss the best strategies for NTM control, we use the effects of NTMs and/or of the auxiliary power required to stabilise them on the factor Q as a global measure of scenario performance. We use a simplified model to determine the burning temperature and total pressure for a given auxiliary power and island width. We start from the so-called scenario 2 of ITER [1], which is the baseline scenario for reaching $Q = 10$ in a sawtoothing ELMy H-mode. The main parameters of interest are: $R_0 = 6.2$m, a = 2m, $\mathrm{I_p} = 15$MA, $\mathrm{B_0} = 5.3$T, V = 830m^3, $\tau_{\mathrm{E0}} = 3.7$s, $\mathrm{Z_{eff}} = 1.7$, $\mathrm{P_{NBI}} = 40$MW, $\mathrm{P}_\alpha = 80$MW, $\mathrm{P_{Brem}} = 21$MW. The scaling law assumed in this case yields $\tau_E \sim P_L^{-e_P}$ with $e_P = 0.69$ and P_L the loss power [1]. The fusion power is given by $P_f = 5P_\alpha$ with:

$$P_\alpha \;=\; \gamma_\alpha \, 1.5\, 10^{-6}\, p_{\mathrm{keV}}^2 \, R(T_{\mathrm{keV}})\, V \;\; [\mathrm{MW}] \tag{2}$$

$$R(T_{\mathrm{keV}}) \;=\; 29.84\, T_{\mathrm{keV}}^{2.5} \, \exp\Big[- \frac{(\mathrm{T_{keV}} + 0.11)^{0.45}}{0.43} \Big], \tag{3}$$

using a useful fit for the reactivity R and where p_{keV} is the total pressure with T expressed in [keV]. The total thermal energy is given by:

$$W_E = \gamma_E \, 3.84\, 10^{-3}\, f_{pe}\, n_{19}\, T_{\mathrm{keV}}\, V \;\; [\mathrm{MJ}] = \mathrm{P_L}\, \tau_{\mathrm{E}}, \tag{4}$$

with $f_{pe} = p/p_e$ and where τ_E can be written as follows using the baseline parameters:

$$\tau_E = \tau_{E0} \left(\frac{P_{L0}}{P_L} \right)^{e_P} \, (1 - \Delta_\tau \, w/a), \tag{5}$$

with w the full island width and Δ_τ given in Eq. (1). For the effective total heating power, we take into acount Bremsstrahlung radiation and the fact that any off-axis additional power is located in a bad confinement region. Therefore we weight its contribution by a profile effect. Assuming steady-state we obtain:

$$P_L = P_\alpha \, + \, P_{NBI} \, + \, (1 - \frac{\rho_s^2}{a^2})\, P_{ec} \, - \, P_{Brem}. \tag{6}$$

In our case, given the position of the 2/1 surface, since the 2/1 mode is the main mode degrading plasma performance, we assume $1 - \rho_s^2/a^2 \approx 0.5$. The radiation term is important to limit the benefits at large temperatures and is taken as follows:

$$P_{Brem} = \gamma_B \, 47.4\, 10^{-6}\, Z_{eff}\, n_{19}^2\, V \, \sqrt{T_{\mathrm{keV}}}. \tag{7}$$

The parameters γ_α, γ_E, γ_B are introduced to take into account the profile effects (since the plasma parameters in the above equations are taken at the plasma center). Assuming a flat density profile and $T(\rho) \sim (1-\rho^2)$ one gets:

$$\gamma_\alpha = 0.19,\ \gamma_E = 0.5,\ \gamma_B = 0.67. \tag{8}$$

From Eq. (4) one obtains:

$$P_L = \left[\frac{\gamma_E\, 2.4\, 10^{-3}\, f_{pe}\, n_{19}\, T_{\rm keV}\, V}{\tau_{E0}\, P_{L0}^{e_P}\, (1-\Delta_\tau\, w/a)}\right]^{\frac{1}{1-e_P}}, \tag{9}$$

which highlights the sensitivity on the power exponent in the scaling law. The burning temperature is then obtained from Eqs. (3, 6, 7) and (9). The measure of the global burning plasma performance, $Q = P_f/(P_{NBI} + P_{ec})$ is then obtained from Eq. (3) at this temperature. We have adjusted the factor $f_{pe} = p/p_e$, total pressure to electron pressure, to 1.83 such as to essentially recover the standard steady-state conditions with no modes ($w = 0$):

$$P_\alpha = 80\text{MW},\ \text{Q} = 10,\ \text{T}_{\rm burn} \approx 20\text{keV},\ \beta_{\rm N} \approx 1.8,\ \text{P}_{\rm Brem} \approx 20\text{MW}, \tag{10}$$

with $P_{NBI} = 40$MW, $\text{P}_{\rm L0} = 99$MW, $\tau_{\rm E0} = \text{HH}\, 3.7$s and $HH = 1$. The HH factor represents any confinement improvement or degradation. With an additional 20MW of EC power, we obtain $P_\alpha = 84$MW and $Q = 7$. In this way we can determine P_α for different HH values and additional P_{ec}, still assuming no NTMs. The results are shown in Fig. 1 for HH values equally spaced between 0.75 and 1.25. This is the operational diagram of interest for the present study. We also show the "anchor" points related to the 3/2 and 2/1 NTMs. If no ECCD is applied, we expect a degradation of 15% (Eq. 1), thus an effective $HH = 0.85$ for the 3/2 mode. Similarly we predict $HH = 0.75$ for the 2/1 mode assuming it does not lock. If it would lock, as predicted in [7] for w >5-10cm, the mode would grow to even larger values and the discharge would probably need to be stopped, although recent results show that the locked mode can be controlled as well [26]. This yields $Q = 6.9$ with a stationary 3/2 mode and $Q = 4.7$ with a 2/1 mode (points A and B in Fig. 1). If the modes are fully stabilized with 20MW and assuming that the EC power needs to be sustained in steady-state, we recover $HH = 1$ but at $P_{ec} = 20$MW, thus $Q \approx 7$. Of course, if the EC power can be switched off, $Q = 10$ is recovered until the next appearance of an NTM if any. Increasing the EC power to stabilise the mode, one will move from points A or B in Fig. 1 to point D

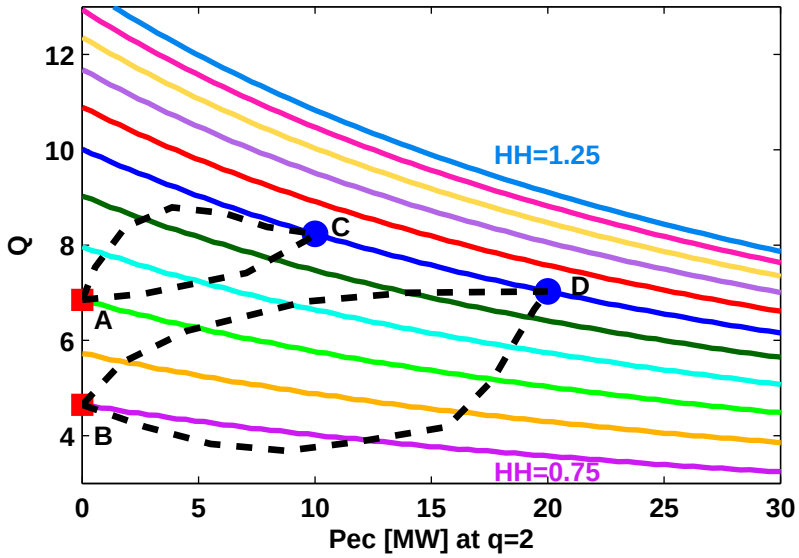

FIG. 1: Q versus additional EC power for HH values between 0.75 and 1.25. The points A and B mark the predicted steady-state performance with either a 3/2 or a 2/1 NTM respectively. The point C and D assumes full stabilisation with constant 10MW or 20MW, respectively, thus are on the curve $HH = 1$. Dashed lines are sketch of possible stationary operating points with a 3/2 or a 2/1 mode partially stabilized.

(or C if 10MW is sufficient to fully stabilise the mode), with a path to be determined and with possible values sketched by the dashed lines. Since the dependence of the saturated island width w_{sat} on P_{ec} can be relatively complex, one might find an optimum Q value at lower values of P_{ec} and thus with a partially stabilised mode. These paths depend on the stabilising parameters and predicted marginal island widths. They will be calculated in Sec. V, but before that, one needs to define the model for calculating $w(P_{ec})$ and to validate it with present experimental results. Depending on effective alignement and assumtions, the mode could be stabilized with 5MW of ECCD power [7]. In such a case, CW would be marginally acceptable sin ce it would yield $Q = 8.9$.

III. STANDARD EQUATIONS FOR COMPARISON WITH EXPERIMENTS

The main characteristics of NTMs which have been observed experimentally are: the proportionality of the saturated island width with poloidal beta, the self-stabilisation at small island width, the confinement degradation (Eq. 1), and the efficient stabilisation with

local ECCD. Other aspects have been observed, but most of them can be included in these global effects. Another important point is the fact that the exact value of the classical tearing parameter related to the total current density profile, $\rho_s\Delta'$, is not easily measured nor well-defined. These characteristics are well encapsulated by the modified Rutherford equation. Since $\rho_s|\Delta'|$ is de facto a free parameter, it is better to normalize the equation for the island growth rate by this value and one obtains the following two basic equations [3, 27]:

$$\frac{\tau_R}{\rho_s^2|\Delta'|}\frac{dw}{dt} = -1 + (1 - \frac{\Delta_\tau w}{a})\,\frac{w_{sat\infty(\beta_p)}\,w}{w^2 + w_{marg}^2} - \tilde{\Delta}'_{cd}, \tag{11}$$

$$\frac{\tau_R}{\rho_s^2|\Delta'|}\frac{dw}{dt} = -1 + (1 - \frac{\Delta_\tau w}{a})\,\frac{w_{sat\infty(\beta_p)}}{w}\,(1 - \frac{w_{marg}^2}{3w^2}) - \tilde{\Delta}'_{cd}, \tag{12}$$

with

$$\tilde{\Delta}'_{cd} = c_j\,(1 - \frac{\Delta_\tau w}{a})\,\frac{w_{sat\infty}}{w_{cd}}\,\frac{j_{cd}}{j_{bs}}\,\eta_{aux}(w/w_{cd}). \tag{13}$$

The left-hand side represents the normalized island growth rate, where τ_R is the resistive time. The first term on the right-hand side is the stabilizing contribution from the equilibrium current density at large island size. The latter is always negative at large island and should depend on w [28]. Here we assume $\rho_s\Delta'$ to be constant and negative, which is reasonable if the ratio between the largest saturated width and the marginal island width is not too large. However, a term like $(1 - \alpha w)$ should replace the term (-1) if the largest saturated width becomes very large [28].

The second term on the right-hand-side is the driving term from the perturbed bootstrap current: $\rho_s\Delta'_{bs}$. It is proportional to $1/w$ at large island size [29] and is reduced at small island size because the effective perturbed bootstrap current is not as large as if the pressure was fully flattened. There are typically two forms which can explain the observed behavior at small island size: Eq. (11) related to the effect of finite $\chi_\perp/\chi_\parallel$ [30], and Eq. (12) related to the effect of the polarisation current [31]. The latter has been assumed in the recent cross-machine analysis [19]. We propose to keep both options, since they have very different behavior at small w, the first one leads to $\rho_s\Delta'_{bs} \sim w$ and the second to $\rho_s\Delta'_{bs} \sim 1/w - 1/w^3$. For full stabilisation with ECCD, this is important because it takes place at small island size. It is argued that using both forms proposed in Eqs. (11, 12) should span the effective dependence of the growth rate at small island width. The latter can indeed be rather

complicated once the effects on the curvature term [32] or of finite orbit width [33], for example, are taken into account. Not that we use the simplest form which still takes the main physical effects. Therefore, for the second model, the frequency dependence is ignored and only the main stabilizing contribution is taken into account with its w dependence. If the latter would decrease due to frequency change, the first model would remain.

The values of $w_{sat\infty}$ and w_{marg} determine the strength of the driving term and of the stabilizing contributions at small island respectively. The first relates to the saturated width at large island size. Indeed, for $w >> 1$, both equations give the same saturated island width, without ECCD contribution:

$$w_{sat}(dw/dt = 0, j_{cd} = 0, w_{marg} \cong 0) = \frac{w_{sat\infty}}{1 + \Delta_\tau \frac{w_{sat\infty}}{a}}, \tag{14}$$

where the denominator includes self-consistently the reduction of β_p due to the NTM and $w_{sat\infty}$ is the saturated island size without confinement degradation nor the stabilizing terms ($w_{sat} >> w_{marg}$, thus the subscript "∞"). The latter can be related to the usual terms of the modified Rutherford equation with:

$$w_{sat\infty} = \rho_s \, \beta_p \, \frac{a_{bs} - a_{ggj}}{\rho_s |\Delta'|}, \tag{15}$$

where the bootstrap and ggj contributions are defined in Ref. [2] and the plasma parameters are taken at the mode onset (or equivalently without the presence of a mode). For cross-machine comparison and prediction to ITER, relatively self-similar plasmas need to be considered (here sawtoothing, ELMy H-modes for scenario 2) and the global β_p is used. This has proven useful and robust in analysing and predicting NTMs behavior in AUG [8], DIII-D [34], JET [3, 35, 36], MAST [37] and TCV [28] with the same method as defined in Refs. [2, 3]. Using ITER scenario 2 parameters, one obtains $w_{sat\infty} = 32$cm from Eq. (15) which leads to a predicted effective stationary saturated island width of 24cm (Eq. 14) once the self-consistent confinement degradation is taken into account. This finally gives an effective confinement degradation of 25%. For the 3/2 mode, we get $w_{sat\infty} = 25$cm and $w_{sat} = 21$cm from Eq. (14) for an effective confinement degradation of 15%. For the 2/1 mode the expected saturated width without EC is larger than the width above which the mode is predicted to lock [7]. We shall discuss the implications in the last Sections. The value here is used to determine the characteristics near full stabilisation.

The marginal island width w_{marg} is the island width at maximum growth rate, without ECCD contribution. Actually, at $max(dw/dt)$ we have $w \simeq w_{marg}(1 - \Delta_\tau w_{marg}/a)$, but

the confinement degradation at $w = w_{marg}$ is less than 5%. Thus, the main characteristics of the modified Rutherford equation are fully determined, without ECCD, once only two parameters are determined, namely $w_{sat\infty}$ and w_{marg}. This is shown in Fig. 2a, where examples of Eqs. (11, 12) are shown, with $j_{cd} = 0$. Dash-dotted lines show the island growth rate without the self-consistent confinement degradation (i.e. assumes $\Delta_\tau = 0$) and therefore the saturated island width is at $w = w_{sat\infty}$ (stable point with $dw/dt = 0$). On the other hand, including the Δ_τ effect (solid lines) modifies the curves at large w and leads to the smaller effective saturated island width w_{sat} (Eq. 14). This is due to the effect of the island on confinement. If a mode onsets at $\beta_p = 0.66$, it will degrade the confinement, β_p will decrease and the mode will not grow to the same size as if additional power would maintain $\beta_p = 0.66$. This stationary effective w_{sat} is directly obtained with the term Δ_τ and fixed onset conditions determine by $w_{sat\infty}$. The curves correspond to the predicted 2/1 mode in ITER Q=10 scenario with $w_{sat\infty} = 32$cm, $w_{sat} = 24$cm, $w_{marg} = 4$cm, and thus $\Delta_\tau\, w_{sat}/a = 25\%$. It is also interesting to note the value of $w_{sat\infty}$ required such that the maximum growth rate is zero, which determines the marginal beta limit [3]:

$$w_{sat\infty,marg} \;=\; 2\, w_{marg} \quad \text{for Eq. (11)}, \tag{16}$$

$$w_{sat\infty,marg} \;=\; 1.5\, w_{marg} \quad \text{for Eq. (12)}. \tag{17}$$

The dashed curves in Fig. 2a have been obtained with $w_{sat\infty}$ set to the above values. In this way, the ratio of $w_{sat\infty}$, measured with the onset β_p, with $2w_{marg}$ or $1.5w_{marg}$ gives the hysteresis factor and is similar to the ratio $\beta_{p,\mathrm{onset}}/\beta_{p,\mathrm{marg}}$.

Experimentally, these two parameters, $w_{sat\infty}$ and w_{marg}, are easily measured. The first one, $w_{sat\infty}$, is measured from the island width w_{sat} when a sufficient β_p is maintained. In this case, the effect of the confinement degradation is not negligible and Δ_τ in Eq. (14) should be taken into account, as seen from Fig. 2a. The second parameter, w_{marg}, is obtained from slow power ramp-down experiments [3, 8] from the island width when the mode quickly self-stabilizes. Note that a very slow decrease of β_p is required to accurately measure w_{marg} [3]. The ratio of $w_{sat\infty}/w_{marg}$ should be of the order of 5 or larger, to ensure an accurate measure of the first parameter. Note that this is often not the case in ECCD experiments, where the saturated island width before the ECCD is applied is often relatively small.

The last term on the right-hand side of Eqs. (11, 12) represents the contribution due to localized ECCD, $\tilde{\Delta}'_{cd} = \Delta'_{cd}/|\Delta'|$ (Eq. 13). Here we assume perfect alignment, while

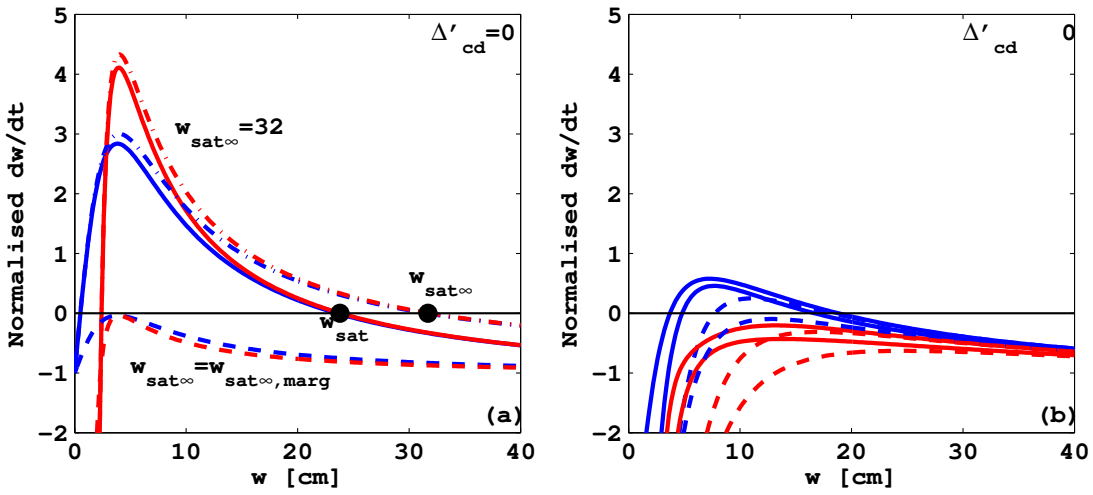

FIG. 2: RHS of Eq.(11) (blue) or Eq. (12) (red) with $w_{marg} = 4$cm, $w_{sat\infty} = 32$cm and $\Delta_\tau = 2.05$. (a) $\Delta'_{cd} = 0$, with (solid) and without (dash-dotted) the term Δ_τ. The dashed lines are obtained with Eq. (17). (b) Same as solid lines of (a) including Δ'_{cd} assuming the 50% or CW with $w_{cd} = 2.5$cm (dashed) or 5cm (solid) and 13.3MW.

misalignment has been taken into account in Refs. [19],[7]. The coefficient c_j is used to fit the experimental results with the above equation. The driven current is assumed to be of the form $j = j_{cd} exp[-4(\rho - \rho_s)^2/w_{cd}^2]$, such that j_{cd} is the peaked currrent density and w_{cd} is the $1/e$ full width. The function $\eta_{aux}(w/w_{cd})$ is related to the stabilizing contribution of the parallel current driven within the island and has typically the following dependence on w ([15], [14], [13], [18]):

$$\eta_{aux,cw}(x = \frac{w}{w_{cd}}) = \frac{1}{1 + 2x^2/3}, \tag{18}$$

$$\eta_{aux,50\%}(x = \frac{w}{w_{cd}}) = \frac{1.8}{x^2} \tanh(\frac{x}{2.5}). \tag{19}$$

The fits are taken from Ref. [18], with a factor 1/2 for Eq. (19) to take into account the effective total driven current and normalised such that $\eta_{aux} \cong 1$ for $w \cong w_{cd}$. The first function, Eq. (18), assumes a localised CW deposition and the second, Eq. (19), a localized deposition near the O-point with 50% modulation. The effect of adding the last term on the right-hand side of Eqs (11, 12) is shown in Fig. 2b. An important characteristic is that the w dependence of η_{aux} is not necessarily the same as the other contributions. Therefore the maximum growth rate might shift to larger values than w_{marg}, which might have important effects when comparing various current density profile widths as will be discussed below.

This is clearly seen in Fig. 2b where we have used the solid line case of Fig. 2a and added Δ'_{cd} with j_{cd}/j_{bs} corresponding to the prediction for ITER with 13.3MW and $w_{cd} = 2.5$cm or 5cm. We see that we can essentially stabilize the mode and that the island width will self-stabilise at about $w = 10$cm (when $max(dw/dt) = 0$). This is indeed 2.5 times larger than w_{marg} and is a realistic situation.

Another form for $\eta_{aux,cw}$ has been used in Ref. [27], $\eta_{aux,fs}$ corresponding to Eq. (20) of [18], but this would not change much the results presented here. It should be noted that in Ref. [18], when assuming a flux surface current density, the author neglected the fact that the phase α_0 in Eq. (19) still depends on the flux surface label ψ. This will in turn define the effective current density inside the island and gives values for η_{aux} in between $\eta_{aux,cw}$ and $\eta_{aux,fs}$, depending on the assumed function $\alpha_0(\psi)$. It is therefore better, for conservative assumptions, to take the form of Eq. (18) which was first calculated in [15]. The differences lie within the error bar of present experimental results and the related predictions that one can draw.

IV. CRITERIA FOR $\eta_{NTM} \equiv j_{cd}/j_{bs}$

Due to the high probability for ITER to have NTMs in its standard scenario [23] and the efficient stabilisation obtained with ECCD [9]-[12], ITER will be equipped with EC upper launchers dedicated mainly to NTM stabilisation. The design of such a launcher tries to maximize the peaked j_{cd} while minimizing the value of w_{cd}. However, to evaluate if a given design is predicted to be able to fully stabilize NTMs in ITER and moreover at what power level, it is useful to have a criteria for $\eta_{NTM} \equiv j_{cd}/j_{bs}$. At present, a criteria of $\eta_{NTM} \geq 1.2$ is used [21], based on Refs. [19, 20]. The latter is obtained assuming 50% modulation and the polarisation model, Eq. (12). It does not take into account the deposition width, w_{cd}, nor the marginal island width w_{marg}. Here, we analyze the effects of these two parameters, in addition to assuming different models for the stabilizing terms at small island width and CW versus 50% modulation. The aim is to obtain a more complete definition of the criteria for η_{NTM} and a well-defined scheme to analize the performance of a given launcher design.

machine	w_{marg}	$w_{sat\infty,\chi}$	$w_{sat\infty,pol}$	j_{cd}/j_{bs}	w_{cd}
AUG	1.5-1.8	3.7	2.9	3.1	1.1
DIII-D	2.5	6.6	5.8	0.9	2.5
JET	4	9.1	8.3	1.2	3.8
JT-60U	4-5	12	10.5	1.2	11.2

TABLE I: Parameters in Eqs. (11, 12) used to determine the values of c_j required in both Eqs. respectively, with $w_{sat\infty,\chi}$ from Eq. (11) and $w_{sat\infty,pol}$ from Eq. (12)

A. Basic ITER parameters used for the study

Before analyzing the criteria for η_{NTM}, one has to determine the basic plasma parameters required in Eqs. (11, 12). That is, the expected values of $w_{sat\infty}$ and w_{marg} and the value of c_j to fit present experiments. The value of Δ_τ is given from the equilibrium used for the ray-tracing simulations. First the coefficient c_j has been determined using the same method as in Ref. [20]. We have obtained the relevant parameters to reproduce the experimental results presented in Ref. [19], using $w_{cd} = 6\delta_{ec}/5$. They are given in Table I. Then, a coefficient c_j is obtained such that all experiments in which full stabilisation is realized lead to $\max(dw/dt) < 0$. Since there are large uncertainties in these early cross-machine comparisons, we have taken "best estimates" for the relevant coefficients. We have taken a conservative value of $c_j = 0.5$ to be used with Eq. (11) and a value of $c_j = 1$ for Eq. (12). Note that we have not considered the effects of local heating within the island, as has been recently observed in TEXTOR [38], nor the effect of j_{cd} on Δ' [39]. These effects should not be dominant in ITER, with good alignment, and they are in fact taken into account, to first order, with the coefficient c_j. In addition to this coefficient, one should take into account the misalignement in the various experiments. However the latter is not yet well determined, therefore the method to determine c_j proposed here can be seen as purposedly conservative for predictions to burning plasmas. We also assume that these coefficients, obtained from 3/2 mode stablisation experiments, are also valid for 2/1 modes.

We now need to determine the plasma parameters expected in ITER. As mentioned earlier, we only need to predict two parameters, namely $w_{sat\infty}$ and w_{marg}. The latter has been predicted to be near 2cm in Ref. [19] and 2-6cm in [3]. We shall use three values,

2, 4 and 6cm in order to study its influence on the predicted results. On the other hand, the value of $w_{sat\infty}$ has not yet been studied systematically across machines, although it would also allow a good test of the theory by comparing with Eq. (15). Therefore we have used the same method as described in Ref. [2] and which has been used to compare with DIII-D [34], JET [3, 35, 36], MAST [37] and TCV [28]. In each cases, the saturated island size was relatively well predicted using global plasma parameters and the formulas in [2]. Using the parameters predicted for the standard scenario in ITER, scenario 2 [1] with $\beta_p = 0.66$ and $\beta_N = 1.8$, we obtain for $q = 2$, a value of $w_{sat\infty} = 32$cm and $\rho_s/a = 0.8$ with $a = 200$cm. The latter yields $\Delta_\tau = 2.05$ and an effective saturated island from Eq. (14) of $w_{sat,2/1,ITER} \simeq 24$cm. Thus, one would have an island of 12% the minor radius and a confinement degradation of 25% with $\beta_N = 1.8$, which looks reasonable when compared with present experimental results with rotating 2/1 modes.

The latest design for the ITER upper launcher [22, 40] has a peaked current density with 13.3MW of $j_{cd} \simeq 0.2\text{MA/m}^2$, such that $\eta_{NTM} \simeq 2.7$, and a width $w_{cd} \simeq d/\sqrt{\kappa} \simeq 2.35$cm, where d is the width defined with respect to the area [40]. The launcher is made of two rows and the other row has a slightly larger value of w_{cd}. This is why we have analyzed the results assuming $w_{cd} = 2.5, 5$ and 10cm in order to see the effects of larger deposition widths. Usually the total driven current is relatively constant, for similar launching conditions. Therefore, when considering various widths, one should keep $(\eta_{NTM}\, w_{cd})$ constant. We shall use $\eta_{NTM}\, w_{cd} = 6.3$ to analyze the present launcher design, which corresponds to the value predicted with 13.3MW (2/3 of the available power).

B. The criteria η_{NTM}

Using the above parameters into Eq. (11) or (12), with different values of w_{marg} (2, 4 or 6cm) and w_{cd} (2.5, 5 or 10cm), we can determine the value of $\eta_{NTM} = j_{cd}/j_{bs}$ such that the NTM is unconditionally stable ($\max(dw/dt) < 0$). These values are given in Tables II and III, with average values given in the bottom two rows. The value of the product $\eta_{NTM} w_{cd}$ is also provided, since it is very useful when comparing various values of w_{cd}. For the present ITER EC upper launcher design [22] with 13.3MW, the expected value of η_{NTM} is 2.52, 1.26 or 0.63 if w_{cd}=2.5, 5 or 10cm respectively. Looking at Tables II and III, we see that for $w_{cd} = 2.5$cm, in 5 cases out of 6 for 50% modulation and 4 out of 6 for CW,

the NTM can be stabilised with the present design of the EC launcher. For $w_{cd} = 5$cm, 2/1 NTMs can be stabilised in 4 out of 6 test cases for both the CW option and the 50% modulation. Finally for $w_{cd} = 10$cm, NTMs cannot be stabilised in CW and marginally for 1 case using 50% modulation (for $w_{marg} = 6$cm). Assuming 20MW, thus $\eta_{NTM} w_{cd} = 9.45$, essentially all cases with $w_{cd} = 2.5$cm or 5cm can be fully stabilised. From tables II and III, we also see that depending on the model the 2/1 mode would be fully stabilised with EC power between 7MW and 20MW. Comparing $w_{cd} = 5$cm with 10cm, we clearly see that localisation is beneficial since the required ($\eta_{NTM} w_{cd}$) values decrease by a factor of two to three and the required η_{NTM} is similar or smaller. On the other hand, when using 2.5cm instead of 5cm, the required values of η_{NTM} increase while the required $\eta_{NTM} w_{cd}$ are similar. This is due to the fact that w_{cd} starts to be of the order of w_{marg}, so there is little gain by reducing it further. Actually, a high degree of radial accuracy is also required for the ECCD deposition location, of the order of w_{cd} or less [7]. Therefore a value of $w_{cd} \approx 5$cm could actually be an optimum.

Tables II and III can be used to compare between the stabilising models. The required values for the "χ_{pol}" model (Eq. (12)) are typically 50%-70% of the ones for the "$\chi_{\perp}$" model (Eq. (11)). However, a large part is due to the lower value of c_j used in Eq. (11) which was very conservative. Using the same value as in Eq. (12) would lead to similar predicted values in both cases. However one needs further detailed experiments to better quantify this value. Finally we can compare the required values assuming CW (Table II) and 50% modulation (Table III). We see that there are actually no significant differences except for $w_{marg} = 2$, since in this case w/w_{cd} can be smaller than one, which is the domain where 50% modulation can be beneficial [12].

The criteria $\eta_{NTM} \geq 1.2$ was essentially based on the "pol" model, Eq. (12), and assuming 50% modulation. With this model, we obtain a similar value, $\eta_{NTM} \geq 1$ from Table III for the cases with $w_{cd} = 5$cm and independently of the value of w_{marg}. However if $w_{cd} = 2.5$cm, then $\eta_{NTM} \geq 1.5$ should be used. Therefore, from Tables II and III we see that a more general criteria should be:

$$w_{cd} \leq 5\text{cm} \quad \text{and} \quad \eta_{NTM}\, w_{cd} \geq 5\text{cm}. \tag{20}$$

	w_{cd} = 2.5cm		w_{cd} = 5cm		w_{cd} = 10cm	
w_{marg}	$\chi_\perp$	χ_{pol}	$\chi_\perp$	χ_{pol}	$\chi_\perp$	χ_{pol}
2 cm	3.7 ; 9.25	1.9 ; 4.75	2.5 ; 12.5	1.7 ; 8.5	4.4 ; 44	3.1 ; 31
4 cm	3.2 ; 8	1.8 ; 4.5	1.9 ; 9.5	1.1 ; 5.5	2.0 ; 20	1.5 ; 15
6 cm	2.6 ; 6.5	1.7 ; 4.25	1.5 ; 7.5	1.0 ; 5	1.3 ; 13	1.0 ; 10
η_{NTM} ; $\eta_{NTM} w_{cd}$	3.17 ; 7.93	1.8 ; 4.5	1.97 ; 9.85	1.27 ; 6.35	2.57 ; 25.7	1.87 ; 18.7
η_{NTM} ; $\eta_{NTM} w_{cd}$	2.49 ; 6.2		1.62 ; 8.1		2.22 ; 22.2	
$\eta_{NTM} w_{cd}$	7.15					

TABLE II: Values of η_{NTM} expected to stabilise 2/1 NTMs on ITER. The first 3 rows correspond to different values of w_{marg}. The columns span the values of w_{cd}=2.5, 5 and 10cm, as well as the two models considered using Eq. (11) for the columns labeled "$\chi_\perp$" and using Eq. (12) for the columns labeled "*pol*". The last two rows yield the average value per model and then per current density width w_{cd}. Table for the CW case, using Eq. (18).

	w_{cd} = 2.5cm		w_{cd} = 5cm		w_{cd} = 10cm	
w_{marg}	$\chi_\perp$	χ_{pol}	$\chi_\perp$	χ_{pol}	$\chi_\perp$	χ_{pol}
2 cm	3.0 ; 7.5	1.5 ; 3.75	2.1 ; 10.5	1.1 ; 5.5	2.0 ; 20	1.1 ; 11
4 cm	2.6 ; 6.5	1.5 ; 3.75	1.7 ; 8.5	1.0 ; 5.0	1.5 ; 15	0.9 ; 9
6 cm	2.1 ; 5.25	1.4 ; 3.5	1.3 ; 6.5	0.9 ; 4.5	1.1 ; 11	0.8 ; 8
η_{NTM} ; $\eta_{NTM} w_{cd}$	2.57 ; 6.43	1.47 ; 3.68	1.7 ; 8.5	1.0 ; 5.0	1.53 ; 15.3	0.93 ; 9.3
η_{NTM} ; $\eta_{NTM} w_{cd}$	2.02 ; 5.05		1.35 ; 6.75		1.23 ; 12.3	
$\eta_{NTM} w_{cd}$	5.9					

TABLE III: Same as Table II but assuming 50% modulation in the O-point, Eq. (19).

V. *Q* PREDICTIONS IN THE PRESENCE OF FINITE WIDTHS NTMS AND EC STABILISATION

The parameters given in Tables II and III define the requirements for full stabilisation. As discussed in Sec. II and shown in Fig. 1, one should consider the effective paths between no stabilisation and full stabilisation in order to determine the best strategy. This is performed

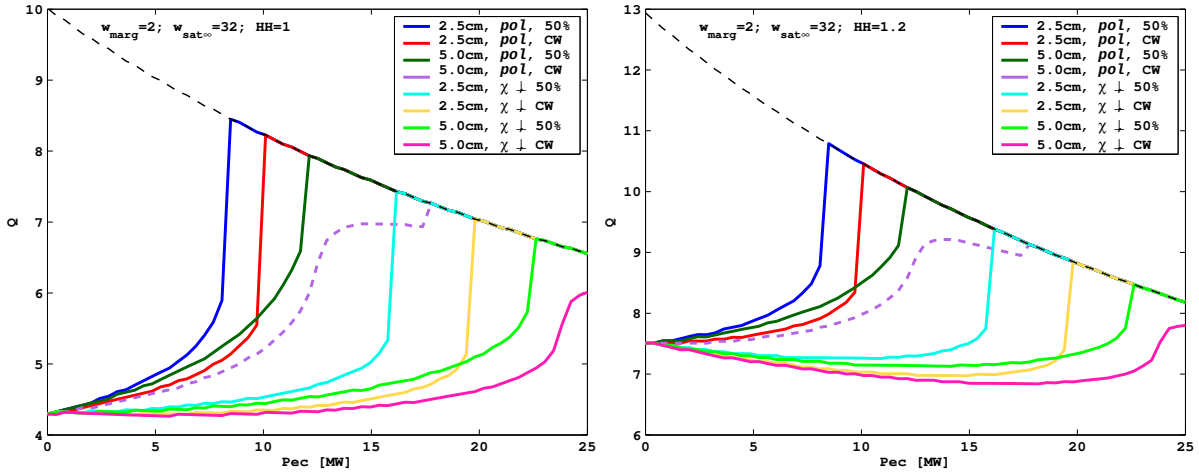

FIG. 3: Q factor obtained with a 2/1 mode controlled with P_{EC} for various models, assuming $w_{marg} = 2$cm, $w_{sat\infty} = 32$cm. The required values for full stabilisation are given in Tables II and III. (a) Assuming $HH = 1$, (b) with $HH = 1.2$.

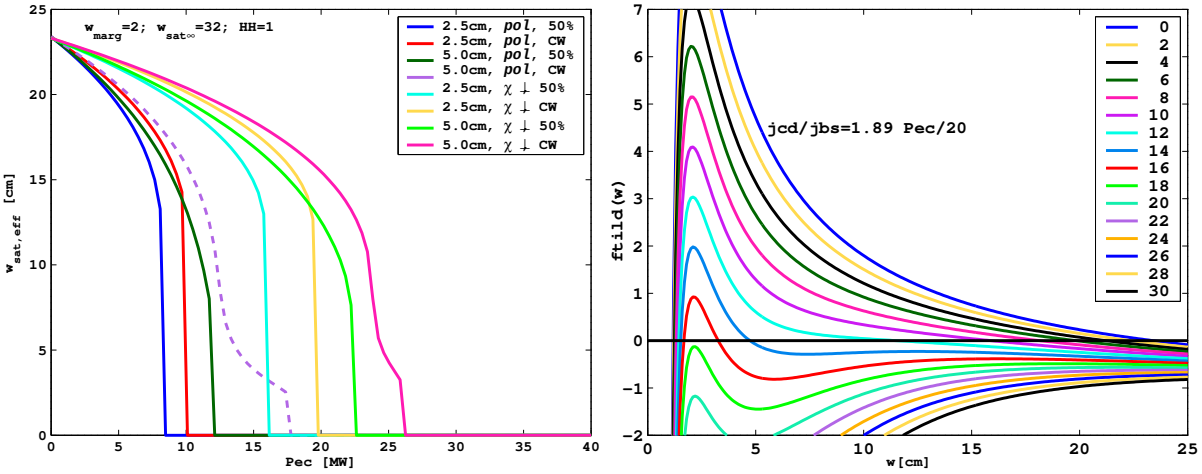

FIG. 4: (a) Effective saturated island width with a given P_{EC} as obtained from Eqs. (11, 12) corresponding to Fig. 3. (b) RHS of Eq. (12) for the case shown with a dashed line in (a) and Fig. 3.

in this Section where we find the effective Q value for a given EC power and current driven, and a resulting saturated island size. In other words we solve Eq. (11) or (12) to determine the saturated island size which determines through Eqs. (1) and (3-9) the resulting Q factor. In this Section we assume that the EC power is turned on all along. The case of stabilizing the mode and then switching off the EC power is considered in the next Section.

We show in Fig. 3 the effective paths of a 2/1 NTM in ITER in the operational diagram

Q versus EC power. We show the eight cases with $w_{marg} = 2$cm and $w_{cd} = 2.5$ or 5cm corresponding to the top row of Tables II and III. The order in the legend corresponds to increasing required ($\eta_{NTM} w_{cd}$) values obtained in Tables II and III for full stabilisation. For example, for $w_{cd} = 2.5$cm, CW and assuming the $\chi_\perp$ model, Table II gives $\eta_{NTM} w_{cd} = 9.25$. Since the UL provide $\eta_{NTM} w_{cd} = 6.3$ for 13.3MW, this means that 19.5MW are required for full stabilisation as confirmed by the sixth trace in Fig. 3(a). Fig. 3(b) shows the similar situation but assuming an improved confinement factor $HH = 1.2$. It should be noted that this only changes the Q values. The former example still stabilizes at 19.5MW, but this time at a Q value of 8.8 instead of 7. The latter effect can be inferred from Fig. 1 as well.

Most cases shown in Fig. 3(a) have a slight Q increase with increasing P_{EC}, until near full stabilisation where $Q(P_{EC})$ increases rapidly. With $HH = 1.2$, many cases have actually Q decreasing first until near full stabilisation. In such cases the best is either full stabilisation or even to keep the mode as such with no EC power, in particular for $HH > 1$. These behaviors can be understood from Fig. 4(a) which shows the predicted w_{sat} versus P_{EC} for these eight cases. We see that the island width does not change much at first with small values of P_{EC}. Therefore there is little gain in confinement and a possible loss due to the additional auxiliary power injected. However when w_{sat} reduces to near 15cm, there is a rapid variation with increasing ECCD. This is because the effective w_{marg} with the Δ'_{cd} term is around 10cm although we have $w_{marg} = 2$cm in the model.

One case has a different behavior, dashed line in Fig. 3, which is the case with $w_{cd} = 5$cm, CW and Eq. (12) (polarisation model). In this case, there is a local maximum of $Q(P_{EC})$ at $P_{EC} < P_{EC,fullstab}$, that is at partial stabilisation. This is of course due to a different dependence of w_{sat} on P_{EC} as seen from Fig. 4(a), dashed line. In this case, w_{sat} decreases rapidly at an intermediate power. To better understand the origin of this behavior, we plot the right-hand side of Eq. (12) with increasing P_{EC} from 0 to 30MW (Fig. 4(b)). With increasing Δ'_{cd}, the growth rate has a relatively flat dependence on w for $w > 5$cm. This is why for a small power increase, for example between 10MW and 14MW, w_{sat} shrinks from 15cm to 5cm (solid circles), yielding a confinement degradation $\Delta_\tau w_{sat}/a$ of 15% down to 5% only. On the other hand, since w_{marg} is small, the peak of the normalized growth rate is still relatively high and one needs an extra 4MW to shrink w_{sat} from 5cm to 2.5cm where it self-stabilizes. These effects could happen more often than expected once all the terms and their various w dependencies are taken into account in the modified Rutherford equation.

It also shows that the dependence of w_{sat} on P_{EC} is not linear nor smooth, and this could complicate some experimental observations.

VI. SAWTEETH AND PRE-EMPTIVE STABILISATION

In the previous Section, we have seen that it is not always the best option, in terms of global instantaneous performance, to fully stabilize an NTM. In this Section we study if it could be beneficial to turn on the EC power only part of the time, in order to reduce the EC energy injected into the plasma and therefore improve the integrated performance. This depends mainly on the frequency of the trigger mechanism, the size of the seed island and on the time it takes to fully stabilize the mode. It could be that the mode is triggered only in the initial phase of the scenario development, due to a first long sawtooth period or a large first ELM as it is seen in JET. In that case, the best strategy is clearly to fully stabilize the mode, with all the power available and then to turn off the EC power while recovering $Q = 10$. Since sawteeth will happen regularly in the stationnary ELMy H-mode scenario 2 case, a regular trigger might occur every sawtooth crash. The sawtooth period can be in between 10s and 100s in ITER, but is hard to predict, and this will influence the best strategy. On the other hand, the time it takes to fully stabilize the mode can be predicted using Eq. (11) or (12) with Eq. (1). This is shown in Fig. 5(a) assuming two seed island sizes of 7cm and 24cm. The first six cases of Fig. 3 are shown, in order of the required $(\eta_{NTM} w_{cd})$ values (Tables II and III), this time for the cases with $w_{marg} = 4$cm. We see that all cases shown can rapidly, within 6s, fully stabilize the mode with 13.3MW if the seed island is about 7cm. However in two cases (which have $(\eta_{NTM} w_{cd}) > 6.3$ in Tables II and III) the mode cannot be stabilized if the seed island is 24cm. Note that it still takes between 27s and 66s to fully stabilize the mode. This can be seen as a reason for the advantage of pre-emptive ECCD (which consists of having EC turned on before the mode is triggered) which will catch the mode in its early stage if it grows from a small island size. Note that the seed island could be created directly at a very large size at the sawtooth crash during the reconnection process as observed sometimes in JET [3]. In that case, pre-emptive ECCD would only be beneficial if it modifies the formation of the seed island during the sawtooth crash.

Another aspect to be taken into account to choose the best strategy on ITER is the fact

that the resistive time is very long as compared with present tokamaks. Therefore the NTM growth is very slow, so one might catch the mode early even if the EC power is turned on only after the mode is detected. This is tested in Fig. 5(b) where a seed island of 7cm is assumed to be triggered at $t = 0$ and then the EC power is turned on at $t = 0, 3$s, 10s, or 20s. The 0s delay would correspond to pre-emptive ECCD, while the other cases to the time it takes to detect the mode, aim at $q = 2$ and turn on the power. A 3s delay time is a reasonable value if the launchers are already aiming at the $q = 2$ surface (from real-time equilibrium and ray-tracing calculations). In this case, three models are displayed, corresponding to the first, fourth and fifth cases shown in Fig. 5(a) (with corresponding colors). With 0s delay, all models can fully stabilize the mode, as seen above. However already with a 3s delay, one model cannot stabilize the mode because of the insufficient value of $(\eta_{NTM} w_{cd})$. If one can fully stabilize the mode, with the other two models shown, then it takes 8-26s if the EC is turned on after 3s, 23-55s if there is a delay of 10s and 39-75s if there is a delay of 20s. These simulations show that there is a large increase in efficiency if the island is catched when it is below about 10-15cm. This relates to the effective marginal island size observed in Sec. V of about 10cm when Δ'_{cd} is included even if $w_{marg} = 2$cm in the model. Another result is that it can easily take more than 20s to fully stabilize the mode. Therefore if the sawtooth period is below about 30s, it is clearly better to keep EC on all the time at either full or partial power depending on the effective Q value obtained. On the other hand, if the sawtooth period is very long, then it might be better to turn on the EC power for a short time of about 10-20s. Actually, real-time measurements and calculations should allow to predict the next sawtooth crash and allow the EC to be turned on just before it occurs, yielding the 0s delay case of Fig. 5(b). This could become the best strategy if the sawtooth period is longer than 30-60s. This is even more true if the mode locks when $w < 5 - 10$cm as predicted in [7]. In that case, it is very important to catch the mode before it grows to that size, although promising stabilization of a locked mode has been recently obtained [26]. From Fig. 5(b), we see that this means the EC power should be active in less than about 3s, which means effectively pre-emptive ECCD.

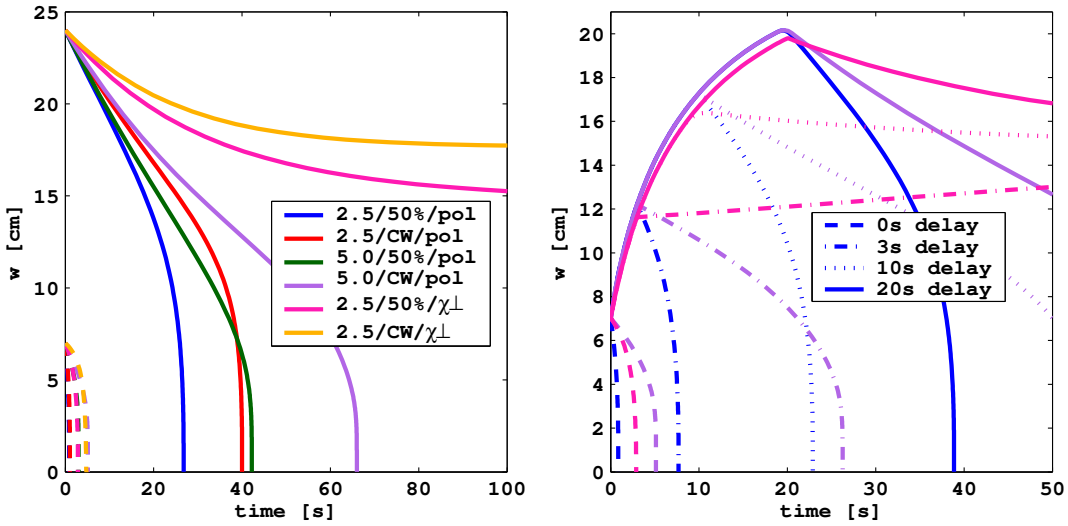

FIG. 5: (a) Time evolution predicted for a 2/1 mode in ITER, assuming a 7cm and a 24cm seed island, using Eqs. (11, 12) with 13.3MW ($\eta_{NTM} w_{cd} = 6.3$) and the models indicated in the legend in order of the required j_{cd} for full stabilisation. (b) Using the 1st, 4th and 5th models of (a), time evolution of a 7cm seed island with 0s, 3s, 10s and 20s delay for the CD term to be included.

VII. CONCLUSIONS

The plasma performance of a burning plasma, characterized by the factor $Q = P_{fusion}/P_{aux}$, is analyzed in details with respect to the presence of neoclassical tearing modes (NTMs). A finite island width leads to a locally enhanced radial transport and to a finite confinement degradation. This effect is proportional to ρ_s^3, where ρ_s is the radius of the $q = m/n$ surface (Eq. 1). Therefore the 2/1 mode, with $\rho_s \approx 0.8$, is the most critical and we have concentrated our study on this mode.

The NTMs can effectively be stabilized by driving local current density within the island [9]-[12]. This shrinks the saturated island and the plasma recovers better confinement. On the other hand, the additional auxiliary power decreases Q (Fig. 1), except if P_{fusion} increases significantly. The effective dependence of Q on P_{EC} for the 2/1 mode on ITER, assuming exact aiming and no mode locking, has been calculated (Sec. V). It is shown that in most cases there is no much gain, or even a decrease of Q, at low P_{EC}, up to near full stabilisation. On the other hand, in some cases partial stabilisation can lead to better Q factor. This is due to a rapid reduction of the island width with small input power, while the peak of the island growth rate, at small island width, still needs significant power to

be decreased below zero. This "non-linear" dependence of w_{sat} on P_{EC} could be observed in present experiments where more stabilizing terms are at play with similar amplitude and different w dependence. This effect could play a role and complicate comparison of experimental results across machines.

A key element in these discussions is of course the power required for full stabilisation. We have analyzed the 2/1 mode predicted in scenario 2 of ITER with respect to two model equations, three different current drive widths, w_{cd}, and three different expected marginal island widths. These model equations, Eqs. (11) and (12), are proposed to be used to compare with present experimental results. They have been written such that only three main parameters ($w_{sat\infty}, w_{marg}$ and c_j) need to be determined and compared with the experimental situation and such that it is most appropriate for analyzing stationnary conditions as obtained experimentally. They represent adequately the driving term (with $w_{sat\infty}$), the plasma stabilising term (w_{marg}) and the effect of EC (with c_j). Note that even though heating effects, CD effects on Δ' and other terms are not explicitely included, they are taken into account implicitely through these three terms. This is especially useful for cross-machine comparisons. We have seen that the comparison of the Δ'_{cd} term with experimental results depends on the model equation used, leading to possibly different matching parameters c_j in Eq. (13).

The required values of j_{cd} for full stabilisation of the 2/1 mode in ITER have been calculated. They are obtained from comparing recent experimental results [19] with Eqs. (11) and (12) and inferring the main parameters $w_{sat\infty}$ and w_{marg} for each machine (Table I). The minimum values of $\eta_{NTM} = j_{cd}/j_{bs}$ and $(\eta_{NTM} w_{cd})$ are provided in Tables II and III. This allows to better check if a given launcher design is able to fully stabilize the 2/1 mode in ITER. For example, the present design yields $\eta_{NTM} \approx 2.5$ for a typical w_{cd} of 2.5cm, giving a value of $\eta_{NTM} w_{cd}$=6.3 with 13.3MW. The tables show that this is sufficient to fully stabilize the mode, even with $w_{cd} = 5$cm to take into account some misalignements of the various beams, especially if 20MW are used. It also shows that a criteria like $\eta_{NTM} \geq 1.2$ is too simple [21] and both η_{NTM} and $(\eta_{NTM} w_{cd})$ need to be considered as well as the various models. The results presented in Tables II and III lead to the criteria (Eq. 20): $w_{cd} \leq 5$cm and $\eta_{NTM} w_{cd} \geq 5$cm.

Fig. 1 shows that full stabilisation with continuous 13.3MW or 20MW leads to a Q of about 7.7 or 7 respectively. Therefore the best strategy cannot be to keep the full power

required to stabilize the mode turned on continuously. The analysis of the time it takes to fully stabilize the mode depending on the seed island width and depending on the delay before the ECCD is turned on at the island location help to determine the best strategies for NTM control. We have shown that if the mode is captured before it reaches about 10cm, then it is much easier to stabilize the mode and much faster. It can be performed in 3-10s, depending on the model. However with a 3-10s delay or if the mode has reached about 20cm, then it can easily take up to 60s to get rid of the mode. Note that it takes 3s for a mode triggered at a seed island size of 7cm to reach 12cm (Fig. 5). This is why pre-emptive ECCD coupled with real-time calculations to determine the time of the next sawtooth crash might be the best strategy to minimize the integrated EC power necessary for NTM control. On the other hand, this will depend on the sawtooth period itself and part of the power might be used to control the sawtooth period. It has been shown in [41] that the sawtooth period can be reduced by about 30% with ECCD well inside the $q = 1$ surface, while it can be increased by 50% with a real-time control algorithm, similar to NTM control, such that the current is driven just outside the $q = 1$ surface with the upper launcher. Thus a combination of sawtooth control and NTM pre-emptive control might be the best. Note that the role of pre-emptive ECCD on the effective size of the seed island triggered at a sawtooth crash after a long sawtooth period has not been studied experimentally yet. This is important to know in order to predict the seed island sizes expected on ITER. The goal of stabilizing/controlling the mode before it reaches 10cm is also in-line with the critical width above which the mode is expected to lock [7]. If it locks, the excursions in confinement (and β, l_i) will be probably too large in a burning plasma and a machine like ITER or DEMO and should be avoided. Therefore pre-emptive ECCD with real-time control to determine when EC will be necessary appear again as the best strategy in order to maximize Q. On the other hand, for the hybrid and advanced scenarios, the main source of NTMs is due to the q and pressure profiles evolution. Therefore in these cases, the EC power might need to be turned on continuously to avoid NTMs and the discussion related to Fig. 1 describes the operational diagram for these scenarios.

The studies presented here show that the requirements to control neoclassical tearing modes in burning plasmas are not just a question of sufficient local current drive capabilities and of aiming at the right position. The role of P_{EC} on Q, the frequency of the trigger events, the size of the seed island, the time it takes to fully stabilize the mode and even the

dependence of the driving and stabilizing terms on the island width play a role in determining the best strategy for NTM control.

References

[1] Progress in the ITER Physics Basis, Nucl. Fusion **47** S1 (2007).

[2] O. Sauter *et al*, Phys. Plasmas **4**, 1654 (1997) and references therein.

[3] O. Sauter *et al*, Plasma Phys. Control. Fusion **44**, 1999 (2002).

[4] Z. Chang and J. D. Callen, Nucl. Fusion **2**, 219 (1990).

[5] R.J. Buttery *et al* Fusion Energy Conf. (Proc. 20th IAEA Conf., Vilamoura, Portugal, 2004) (Vienna, IAEA, 2004), paper IAEA-CN-116/EX/7-1

[6] T. C. Hender *et al*, Nucl. Fus. **44**, 778 (2004).

[7] R. La Haye *et al*, Nucl. Fus. **49**, 045005 (2009).

[8] M. Maraschek *et al*, Plasma Phys. Contr. Fus. 45 (2003) 1369.

[9] G. Gantenbein *et al*, Phys. Rev. Lett. **85**, 1242 (2000).

[10] R. J. La Haye *et al*, Phys. Plasmas **9**, 2051 (2002).

[11] A. Isayama *et al*, Nucl. Fusion **47**, 773 (2007).

[12] M. Maraschek *et al*, Phys. Rev. Lett. **98** (2007) 025005.

[13] C.C. Hegna, J.D. Callen, Phys. Plasmas **4**, 2940 (1997).

[14] H. Zohm, Phys. Plasmas **4**, 4333 (1997).

[15] F. W. Perkins *et al*, in Proceedings of the 24th European Conference on Contr. Fusion and Plasma Phys., Berchtesgaden, 1997, (European Physical Society, Petit Lancy, 1997), Europhys. Conf. Abstr. **21A**, 1017.

[16] G. Giruzzi *et al*, Nucl. Fusion **39**, 107 (1999).

[17] G. Ramponi *et al*, Phys. Plasmas **6**, 3561 (1999).

[18] O. Sauter, Phys. Plasmas **11**,4808 (2004).

[19] R. La Haye *et al*, Nucl. Fus. **46**,451 (2006).

[20] H. Zohm *et al*, 14th Workshop on ECE and ECRH, Santorini, Greece May, 2006.

[21] G. Saibene *et al*, Fusion Energy Conf. (Proc. 21st IAEA Conf., Chengdu, 2006) (Vienna, IAEA, 2006), paper IT/P2-14.

[22] M. A. Henderson *et al*, ibidem [21], paper IT/P2-15.

[23] O. Sauter *et al*, Phys. Rev. Lett. **88**, 105001 (2002).

[24] F. Porcelli *et al*, Plasma Phys. Control. Fusion **38**, 2163 (1996).

[25] L.-G. Eriksson *et al*, Phys. Rev. Lett **92**, 235004 (2004).

[26] F. A. G. Volpe *et al*, Phys. Plasmas **16**, 102502 (2009).

[27] O. Sauter *et al*, ibidem [21], paper TH/P3-10.

[28] H. Reimerdes *et al*, Phys. Rev. Lett **88**, 105005 (2002).

[29] R. Carrera *et al*, Phys. Fluids 29 (1986) 899.

[30] R. Fitzpatrick, Phys. Plasmas **2**, 825 (1995).

[31] A. B. Mikhailovskii, Contrib. Plasma Phys. **43**, 125 (2003) and references herein.

[32] H. Lütjens, J.-F. Luciani and X. Garbet, Phys. Plasmas **8**, 4267 (2001).

[33] E. Poli *et al*, Phys. Rev. Lett. **88**, 075001 (2002).

[34] R. J. La Haye, O. Sauter, Nucl. Fus. **38**, 987 (1998).

[35] G. T. A. Huysmans *et al*, Nucl. Fusion, **39** 1965 (1999).

[36] R. J. Buttery *et al*, Plasma Phys. Control. Fusion **42**, B61 (2000).

[37] R. Buttery *et al*, Phys. Rev. Lett. **88**, (2002).

[38] E. Westerhof *et al*, Nucl. Fus. **47**, 85 (2007).

[39] R. J. La Haye *et al*, Nucl. Fus. **48**, 054004 (2008).

[40] G. Ramponi *et al*, Nucl. Fusion, **48**, 054012 (2008).

[41] C. Zucca, *Modeling and control of the current density profile in tokamaks and its relation to electron transport*, PhD Thesis No. 4360, EPFL, Lausanne, 2009. http://library.epfl.ch/theses/?nr=4360.